



MHD CONVECTIVE HEAT TRANSFER THROUGH A HORIZONTAL WAVY CHANNEL WITH HEAT ABSORPTION/GENERATION-A NUMERICAL ANALYSIS

C. G. Jagannatha, Assistant Professor, Department of Mathematics, Government Science college Chitradurga, Karnataka

Naveen Kumar N P, Associate Professor, Department of Mathematics, Government First Grade College, Malleshwaram, Karnataka

Dinesh Kumar S. T., Associate Professor, Department of Mathematics, Government Science college Chitradurga, Karnataka

ABSTRACT

The controlling of heat transport procedures through external energy source effects is one of the mainly significant problems in modern applied physical sciences. Major strong research in thermal sciences, mechanical engineering and including energy modeling, planning and energy supervisions, energy conservations, energy efficiencies, biomass and bio-energy, renewable energy, energy storage, energy in buildings. In the current existing paper, the consequences of thermal conductivity on temperature, this is inversely proportionally by the linear function of temperature on free convective movement of an incompressible viscous fluid through the heated uniform and vertical wavy surface is examined. The dimensionless governing coupled unsteady boundary layer partial differential equations are solved by the Laplace transform technique.

The velocity and temperature profiles were plotted and their behavior is discussed in detail. The Stress and the average Nusselt number are also calculated and tabulated for these sets of parameters.

Key words: Heat transfer, Radiation effect, Wavy channel, Oscillatory flux

1. Introduction:

Unsteady convection flows play an important role in aerospace technology, turbo-machinery and chemical Engineering. Such flows arise due to either unsteady motion of boundary or boundary temperature. Unsteadiness may also be due to oscillatory free stream velocity or temperature. These oscillatory free convective flows are important from technological point of view.

The heat transfer through wavy channels has been a topic of interest in recent times owing to its applications in technological areas viz., transpiration cooling of re-entry vehicles and rocket boosters, cross-hatching of an ablative surface and film vaporization in combustion chambers.

The magneto hydrodynamic (MHD) is a subdivision of fluid dynamics and this studied the association of the electrically conducting fluids in the magnetic field. Many of investigative efforts in the MHD has been proceed extensively for the duration of the preceding little decades subsequent to the established work of Hartmann [1] in fluid metalized ducts flow under external magnetic field. There are most applications for the parabolic movement for instance solar cooker, solar concentrator and parabolic through stellar collector. The parabolic concentrator model solar cookers have the wide range of applications for example baking, roast as well as distillations. Solar concentrator model had those applications into growing rates of evaporations in dissipate stream, in food dispensations, for producing consumption water from salt water as well as seawater. Murthy et al. [2] discussed by the evaluations of thermal performances of temperature exchangers units for parabolic solar cookers. Raja et al. [3] explored the designing as well as manufacturing of parabolic during solar collector systems. Muthucumaraswamy and Geetha [4] discussed the impacts of parabolic movement on the isothermal perpendicular plates by the invariable mass flux. Akbar et al. [5] considered the MHD stagnation point flow of Carreau fluid towards the porous shrinking sheet. Sheikholeslami et al. [6] discussed the magnetic field effects on nanofluid flows as well as temperature transportation. Magnetic field effects on unsteady nanofluid flow as well as temperature transportation utilizing the Buongiorno modeling has been discussed by Sheikholeslami et al. [7]. Sheikholeslami et al. [8] explored the unsteady MHD liberated convective stream in the eccentric semi-annulus packed by the



nanofluids. Sheikholeslami as well as Ellahi [9] explored the 3D meso-scopic simulation of magnetic field effects on nanoliquids. Sheikholeslami et al. [10] defined the solution of forced convective temperature transportation by the changeable magnetic fields. Sheikholeslami and Chamkha [11] studied the free convective temperature transportation of the nanoliquids into the half-annulus enclosures by the sinusoidal walls.

Magnetic field plays an important role in numerous fields such as biological, chemical, mechanical and medical research. In clinical and medical research the magnets are extremely important to create three dimensional images of anatomical and diagnostic importance from nuclear magnetic resonance signals. In view of these applications, the present research is to the effects of radiation on magneto hydrodynamic (MHD) flow and heat transfer problem has become innovative and significant industrially. At high functioning of heat and radiation impact might be moderately momentous. Numerous processes in manufacturing regions occur at huge temperature and consideration of radiation heat transport becomes extremely significant for the construction of the significant apparatus. Nuclear energy plants, some gas turbines and the different propulsion machines for satellites, missiles, aircraft, and space vehicles are illustrations of several engineering regions [12].

Recently, Syed et al. [13] discussed the significances of non-uniform heat generation/absorption in hydromagnetic flow of nanofluid due to stretching/shrinking disk. Saleem and Heidarshenas [14] explored an investigation on exergy in a wavy wall micro channel heat sink by using various nano particles in fluid flow. Nazeer et al. [15] explored heat and mass transfer of Couples stress fluid treated as physiological fluid and caused due to metachronal wave induced by the coincident oscillation of a tiny hair-like structure. Al-Zubaidi et al. [16] discussed the thermal analysis of blood flow of Newtonian, pseudo-plastic and dilatant fluids through an inclined wavy channel due to metachronal wave of cilia. Nazeer et al. [17] explored the numerical solution of gyrotactic microorganism flow of nanofluid over a riga plate with the characteristic of chemical reaction and convective condition. Kiranakumar et al. [18] provided an overview of electrical and gas-sensing properties of reduced graphene oxide–metal oxide nano-composites with improved sensitivity, selectivity, stability, and other sensing performances. Khan et al. [19] investigated the novel characteristics of entropy generation in nonlinear mixed convective flow of nanofluid between two stretchable rotating disks. A new chemical reaction model for rheological relations of Maxwell fluids comprising both heat and mass transfer expressions

Simultaneously has been discussed by Khan et al. [20]. The MHD stagnation point flow of Carreau fluid in presence of heterogeneous, homogeneous reactions with nonlinearly stretching, variable sheet thickness and convective boundary condition has been explored by Hayat et al. [21]. Hayat et al. [22] studied the MHD two-dimensional flow of Eyring-Powell fluid with thermo phoresis and Brownian motion due to convection type stretching cylinder with thermal radiation and heat source/sink. The blood flow in the presence of hybrid nano particles through a tapered complex wavy curved channel is numerically investigated by Abbasi et al. [23]. Vajravelu and Prasad [24] presented the current theoretical developments and applications of the Keller-box method to nonlinear problems. They have given a number of examples of coupled nonlinear problems that have been solved by means of the Keller-box method. The particular area of focus is on fluid flow problems governed by nonlinear equation. To this end the full Keller box method is approached in stages beginning with the standard Newton Raphson method and/or Newton's quasi-linearization methodology solving the root of one algebraic equation. This is extended to two and more variables, and subsequently to ordinary differential equations. Finally, as if an extra do loop were to be added in, we obtain the Keller box method for solving parabolic systems of partial differential equations.

In this paper we investigate the effect or radiation on unsteady convective heat transfer flow of a viscous fluid through a horizontal wavy channel. By using a regular perturbation method the non-linear coupled equations of flow and heat transfer are solve. The effect of radiation on flow and heat transfer characteristics is discussed in detail.

II. Formulation of the problem

We consider the unsteady motion of a viscous, incompressible electrically conducting fluid through a porous medium in a horizontal channel bounded by wavy walls in the presence of a constant heat source /sink. A uniform magnetic field of strength 'Ho' is applied normal to the walls. The Boussinesq approximation is used so that the density variation will be considered only in the buoyancy force. The viscous, Darcy and Ohmic dissipations are neglected in comparison to the flow by conduction and convection. Also the kinematic viscosity ν , the thermal conducting k are treated as constants. We choose a rectangular Cartesian system $O(x, y)$ with x -axis in the direction of motion and y -axis in the vertical direction and the walls are taken at $y = \pm Lf(\delta x/L)$, where $2L$ is the distance between the walls, f is a twice differentiable function and δ is a small parameter proportional to the boundary slope. A linear density temperature variation is assumed with ρ_e and T_e are the density and temperature in the equilibrium state. The magnetic Reynolds number R_m is chosen to be much less than unity so that the induced magnetic field can be neglected in comparison to the applied field. The flow is maintained by an oscillatory volume flux rate for which a characteristic velocity is defined as

$$q(1 + ke^{i\omega t}) = \left(\frac{1}{L}\right) \int_{-Lf}^{Lf} u dy \quad (2.1)$$

The equations governing the unsteady magneto hydrodynamic flow and heat transfer in Cartesian coordinate system $O(x,y,z)$, in the absence of any input electric field are

Equation of continuity

$$\frac{\partial u}{\partial x} + \frac{\partial v}{\partial y} = 0 \quad (2.2)$$

Equation of linear momentum

$$\rho_e \left(\frac{\partial u}{\partial t} + u \frac{\partial u}{\partial x} + v \frac{\partial u}{\partial y} \right) = -\frac{\partial p}{\partial x} + \mu \left(\frac{\partial^2 u}{\partial x^2} + \frac{\partial^2 u}{\partial y^2} \right) - \left(\frac{\sigma \mu_e^2 H_o^2}{\rho_e} \right) u \quad (2.3)$$

$$\rho_e \left(\frac{\partial v}{\partial t} + u \frac{\partial v}{\partial x} + v \frac{\partial v}{\partial y} \right) = -\frac{\partial p}{\partial y} + \mu \left(\frac{\partial^2 v}{\partial x^2} + \frac{\partial^2 v}{\partial y^2} \right) - \rho g \quad (2.4)$$

Equation of energy

$$\rho_e C_p \left(\frac{\partial T}{\partial t} + u \frac{\partial T}{\partial x} + v \frac{\partial T}{\partial y} \right) = \lambda \left(\frac{\partial^2 T}{\partial x^2} + \frac{\partial^2 T}{\partial y^2} \right) + Q - \frac{\partial(q_r)}{\partial y} \quad (2.5)$$

Equation of state

$$\rho - \rho_e = -\beta \rho_e (T - T_e) \quad (2.6)$$

In the equilibrium state

$$0 = -\frac{\partial p_e}{\partial x} - \rho_e g \quad (2.7)$$

Where $p = p_e + p_D$, p_D being the hydrodynamic pressure and in this state the temperature gradient balances the heat flux generated by source Q .

The flow being two-dimensional, in order to maintain the compatibility of the equations (2.4) and (2.6) the temperature in the flow field must be a general function of x and y . However temperature over the boundary walls may be kept constant assuming the temperature dependence on the walls to be a function of $\eta = y/f(x)$.

The boundary conditions for the velocity and temperature fields are

$$\begin{aligned} u=0, v=0, T=T_1(\eta) \text{ on } y=-L f(\delta x/L) \\ u=0, v=0, T=T_2(\eta) \text{ on } y=L f(\delta x/L) \end{aligned} \quad (2.8)$$

Invoking Rosseland approximation (Brewster(1a)) for the radiative flux we get

$$q_r = \frac{4\sigma}{3\beta_R} \frac{\partial(T'^4)}{\partial y} \quad (2.9)$$

expanding T'^4 in Taylor series about T_e and neglecting higher order terms

$$T'^4 \approx 4TT_e^3 - 3T_e^4 \quad (2.10)$$

In view of the continuity equation (2.3) we define the stream function ψ as

$$u = \frac{\partial\psi}{\partial y}, \quad v = -\frac{\partial\psi}{\partial x} \quad (2.11)$$

Eliminating pressure p from equations (2.3) & (2.4) and using (2.11) the equations governing the flow in terms of ψ are

$$[(\nabla^2\psi)_t + \psi_x(\nabla^2\psi)_y - \psi_y(\nabla^2\psi)_x] = \nu\nabla^4\psi + \beta g(T - T_0)_x - \left(\frac{\sigma\mu_e^2 H_o^2}{\rho_e}\right) \frac{\partial^2\psi}{\partial y^2} \quad (2.12)$$

$$\rho_e C_p \left(\frac{\partial T}{\partial t} + \frac{\partial\psi}{\partial y} \frac{\partial T}{\partial x} - \frac{\partial\psi}{\partial x} \frac{\partial T}{\partial y} \right) = k_1 \nabla^2\theta + Q + \frac{16T_e^3\sigma^*}{3\beta_R} \frac{\partial^2 T}{\partial y^2} \quad (2.13)$$

Introducing the non-dimensional variables in (2.12) & (2.13) as

$$x' = x/L, \quad y' = y/L, \quad t' = t\varpi, \quad \Psi' = \Psi/qL, \quad \theta = \frac{T - T_e}{T_2 - T_e} \quad (2.14)$$

the governing equations in the non-dimensional form (after dropping the dashes) are

$$\gamma^2 ((\nabla^2\psi)_t + R \frac{\partial(\psi, \nabla^2\psi)}{\partial(x, y)}) = \nabla^4\psi + \left(\frac{G}{R}\right)\theta_x - M^2 \frac{\partial^2\psi}{\partial y^2} \quad (2.15)$$

and the energy equation in the non-dimensional form is

$$P_1\gamma^2 \left(\frac{\partial\theta}{\partial t}\right) + P_1R \left(\frac{\partial\psi}{\partial y} \frac{\partial\theta}{\partial x} - \frac{\partial\psi}{\partial x} \frac{\partial\theta}{\partial y}\right) = \nabla^2\theta + \alpha_1 \quad (2.16)$$

with the corresponding boundary conditions

$$\psi(+1) - \psi(-1) = (1 + ke^{i\varpi})$$

$$\frac{\partial\psi}{\partial x} = 0, \quad \frac{\partial\psi}{\partial y} = 0, \quad \theta = \frac{T_1 - T_e}{T_2 - T_e} = h, \text{ say} \quad \text{on } y = -f(\delta x)$$

$$\frac{\partial\psi}{\partial x} = 0, \quad \frac{\partial\psi}{\partial y} = 0, \quad \theta = 1 \quad \text{on } y = f(\delta x)$$

$$\frac{\partial\theta}{\partial y} = 0, \quad \text{at } y = 0 \quad (2.17)$$

Where

$$R = \frac{qL}{\nu} \quad (\text{The Reynolds number})$$

$$G = \frac{\beta g(T_2 - T_e)L^3}{\nu^2} \quad (\text{The Grashof number})$$

$$P = \frac{\mu C_p}{k_1} \quad (\text{The Prandtl number})$$

$$M^2 = \left(\frac{\sigma\mu_e^2 H_o^2 L^2}{\nu^2}\right) \quad (\text{The Hartman number})$$

$$\gamma^2 = \left(\frac{\varpi L^2}{\nu} \right) \quad \text{(The wormeley number)}$$

$$\alpha = \frac{QL^2}{k} \quad \text{(The Heat source parameter)}$$

$$N = \frac{4\sigma^* T_e^3}{\beta_R k_1} \quad \text{(The radiation parameter)}$$

$$P_1 = \frac{3NP}{3N + 4}, \quad \alpha_1 = \frac{3N\alpha}{3N + 4}$$

III. Analysis of the flow.

Introduce the transformation such that

$$\bar{x} = \delta x, \quad \frac{\partial}{\partial x} = \delta \frac{\partial}{\partial \bar{x}}$$

Then

$$\frac{\partial}{\partial x} \sim O(\delta) \rightarrow \frac{\partial}{\partial \bar{x}} \sim O(1)$$

For small values of $\delta \ll 1$ the flow develops slowly with axial gradient of order δ and hence we take

$$\frac{\partial}{\partial \bar{x}} \sim O(1).$$

Using the above transformation the equations (2.15) & (2.16) reduce to

$$\gamma^2 ((F^2 \psi)_t + R \frac{\partial(\psi, F^2 \psi)}{\partial(x, y)}) = F^4 \psi + \left(\frac{\hat{G}}{R}\right) \theta_x - M^2 \frac{\partial^2 \psi}{\partial y^2} \quad (3.1)$$

$$P_1 \gamma^2 \left(\frac{\partial \psi}{\partial t}\right) + \delta P_1 R \left(\frac{\partial \psi}{\partial y} \frac{\partial \theta}{\partial x} - \frac{\partial \psi}{\partial x} \frac{\partial \theta}{\partial y}\right) = F^2 \theta + \alpha_1 \quad (3.2)$$

where

$$F^2 = \delta^2 \frac{\partial^2}{\partial \bar{x}^2} + \frac{\partial^2}{\partial y^2}, \quad \bar{G} = G\delta$$

The flow develops slowly with axial gradient of order δ and hence we take $\frac{\partial}{\partial \bar{x}} \sim O(1)$.

We may note that the maintenance of slowly varying axial boundary temperature gives rise to the convection currents and in view of the compatibility at the zeroth order level the analysis is valid provided the thermal buoyancy parameter $G \sim O(1)$ implying $\hat{G} \sim O(1)$.

We adopt the perturbation scheme and write

$$\begin{aligned} \psi(x, y) &= (\psi_0 + ke^{it} \bar{\psi}_0) + \delta(\psi_1 + ke^{it} \bar{\psi}_1) + \dots \\ \theta(x, y) &= (\theta_0 + ke^{it} \bar{\theta}_0) + \delta(\theta_1 + ke^{it} \bar{\theta}_1) + \dots \end{aligned} \quad (3.3)$$

On substituting (3.3) in (3.1) - (3.2) and separating the like powers of δ the equations and respective conditions to the zeroth order are

$$\theta_{0,\eta\eta} = -\alpha_1 f^2 \quad (3.4)$$

$$\psi_{0,\eta\eta\eta\eta} - M_1^2 \psi_{0,\eta\eta} = -\left(\frac{\hat{G}}{R} f^3\right) \theta_{0,\bar{x}} \quad (3.5)$$

$$\bar{\theta}_{0,\eta\eta} - (i\gamma^2 f^2)\bar{\theta}_0 = 0 \quad (3.6)$$

$$\bar{\psi}_{0,\eta\eta\eta\eta} - (M_1^2 + i\gamma^2)f^2\bar{\psi}_{0,\eta\eta} = -\left(\frac{\hat{G}}{R}f^3\right)\bar{\theta}_{0,x} \quad (3.7)$$

$$\theta_0(+1) = 1, \theta_0(-1) = h \quad (3.8)$$

$$\psi_o(+1) - \psi_o(-1) = 1, \psi_{0,\eta}(\pm 1) = 0, \psi_{0,x}(\pm 1) = 0 \quad (3.9)$$

$$\bar{\theta}_o(\pm 1) = 0, \quad (3.10)$$

$$\bar{\psi}_o(+1) - \bar{\psi}_o(-1) = 1, \bar{\psi}_{0,\eta}(\pm 1) = 0, \bar{\psi}_{0,x}(\pm 1) = 0 \quad (3.11)$$

The equations to the first order are

$$\theta_{1,\eta\eta} = -(P_1 R f^2)(\psi_{0,\eta}\theta_{0,x} - \psi_{0,x}\theta_{0,\eta}) \quad (3.12)$$

$$\psi_{1,\eta\eta\eta\eta} - (M_1^2 f^2)\psi_{1,\eta\eta} = -\left(\frac{\hat{G}}{R}f^3\right)(\theta_{1,x}) + Rf(\psi_{o,\eta}\psi_{o,x\eta\eta} - \psi_{o,x}\psi_{0,\eta\eta\eta} - \left(\frac{2f'}{f}\right)\psi_{0,\eta}\psi_{o,\eta\eta}) \quad (3.13)$$

$$\bar{\theta}_{1,\eta\eta} - (iP_1\gamma^2 f^2)\bar{\theta}_1 = (P_1 R f^2)(\psi_{0,\eta}\bar{\theta}_{0,x} - \psi_{0,x}\bar{\theta}_{0,\eta} + \bar{\psi}_{0,x}\theta_{o,\eta}) \quad (3.14)$$

$$\bar{\psi}_{1,\eta\eta\eta\eta} - (M_1^2 f^2)\bar{\psi}_{1,\eta\eta} = -\left(\frac{\hat{G}}{R}f^3\right)(\bar{\theta}_{1,x}) + Rf(\bar{\psi}_{o,\eta}\psi_{o,x\eta\eta} - \psi_{o,x}\bar{\psi}_{0,\eta\eta\eta} + \psi_{o,\eta}\bar{\psi}_{o,x\eta\eta} - \bar{\psi}_{o,x}\psi_{0,\eta\eta\eta}) \quad (3.15)$$

The corresponding boundary conditions are

$$\theta_1(+1) = 0, \quad \theta_1(-1) = 0 \quad (3.16)$$

$$\psi_1(+1) - \psi_1(-1) = 0, \psi_{1,\eta}(\pm 1) = 0, \psi_{1,x}(\pm 1) = 0 \quad (3.17)$$

$$\bar{\theta}_1(\pm 1) = 0 \quad (3.18)$$

$$\bar{\psi}_1(+1) - \bar{\psi}_1(-1) = 0, \bar{\psi}_{1,\eta}(\pm 1) = 0, \quad \bar{\psi}_{1,x}(\pm 1) = 0 \quad (3.19)$$

IV. Shear Stress and Nusselt Number

The shear stress on the channel walls is given by

$$\tau = \frac{\sigma_{xy}(1 - f'^2) + (\sigma_{yy} - \sigma_{xx})f'^2}{(1 + f'^2)}$$

where

$$\sigma_{ij} = -p\delta_{ij} + 2\mu e_{ij}$$

$$\sigma_{xx} = \frac{\partial u}{\partial x}, \sigma_{yy} = \frac{\partial v}{\partial y}, \sigma_{zz} = \frac{\partial w}{\partial z}, \sigma_{xy} = 0.5\left(\frac{\partial u}{\partial y} + \frac{\partial v}{\partial x}\right)$$

and the corresponding expressions are

$$(\tau)_{\eta=+1} = ((1 - f'^2)f^2(e_{48} + ke^{it}e_{50}) + \delta((1 - f'^2)f^2(g_{21} + ke^{it}g_{10}) - (\frac{2f'}{f})(g_{25} + ke^{it}g_{26}) + O(\delta^2)))/(1 + f'^2)$$

$$(\tau)_{\eta=-1} = ((1 - f'^2)f^2(e_{49} + ke^{it}e_{50}) + \delta((1 - f'^2)f^2(g_{22} + ke^{it}g_{20}) - (\frac{2f'}{f})(g_{29} + ke^{it}g_{31}) + O(\delta^2)))/(1 + f'^2)$$

The local rate of heat transfer coefficient (Nusselt number Nu) on the walls has been calculated using the formula

$$Nu = \frac{1}{f(\theta_m - \theta_w)} \left(\frac{\partial \theta}{\partial y} \right)_{\eta=\pm 1}$$

where

$$\theta_m = 0.5 \int_{-1}^1 \theta dy$$

and the corresponding expressions are

$$(Nu)_{\eta=+1} = \frac{2(e_{40} + \delta(e_{41} + ke^{it}e_{42}))}{f(e_3 + \delta(e_{38} + ke^{it}e_{39}) - 1)}$$

$$(Nu)_{\eta=-1} = \frac{2(e_{43} + \delta(e_{44} + ke^{it}e_{45}))}{f(e_{37} + \delta(e_{38} + ke^{it}e_{39}) - h)}$$

where $e_1, e_2, \dots, e_{40}, \dots, e_{50}, g_1, g_2, \dots, g_{31}$ are constants

V. Analysis of the Numerical results

The primary aim of our analysis is to investigate the radiation effect on the behavior of the temperature induced buoyancy force taking in to account the effect of surface geometry and wall temperature ratio. To expand a viewpoint of the physics of the flow regime, we have numerically evaluated the effects of the Hartmann number (M), Grashof number (Gr), radiation conduction parameter (R), dimensionless time (t), and porosity parameter (K) on the velocity components u and v, temperature θ , concentration -, shear stress, Nusselt number, and Sherwood number. Here we consider $Gr = 3, Gm = 5 > 0$ (cooling of the plate), i.e., free convection currents convey heat away from the plate into the boundary layer, and $t = 1, R = 1$ throughout the discussion.

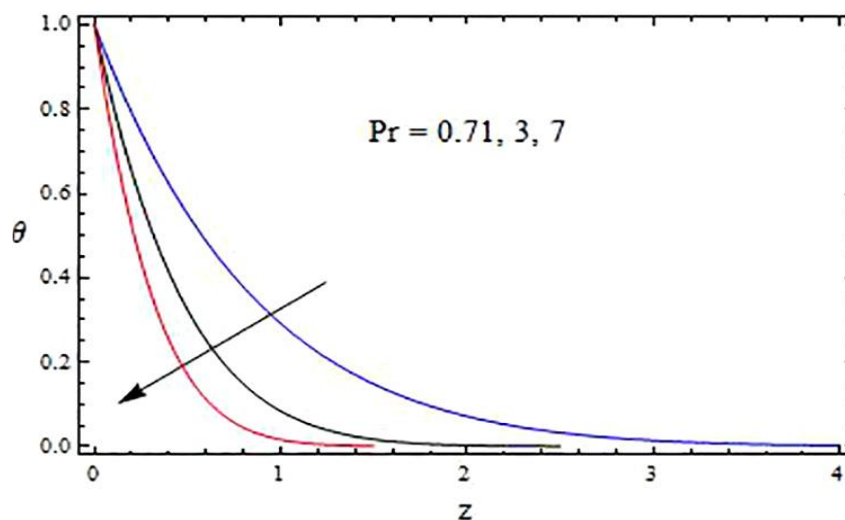


Fig. 1: The temperature profile for θ against Pr with $R = 0.5, t = 1$

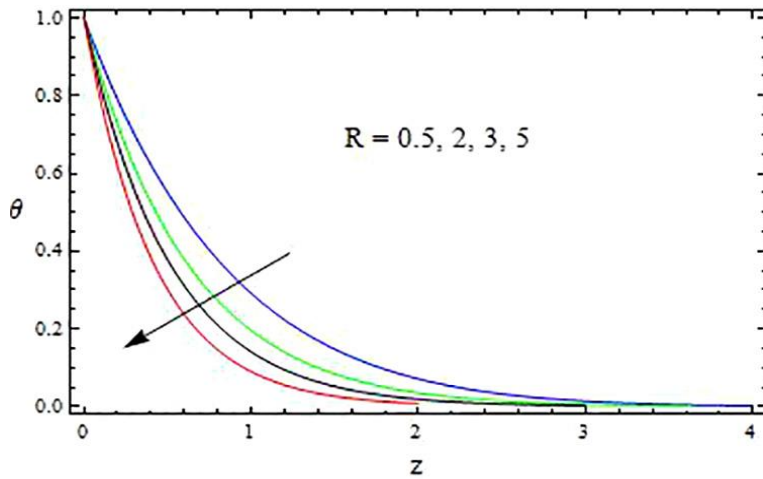


Fig. 2: The temperature profile for θ against R

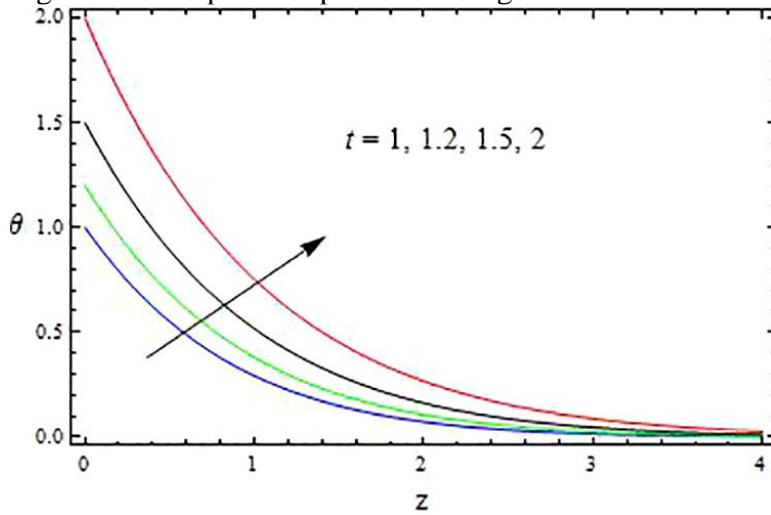


Fig. 3: The temperature profile for θ against t

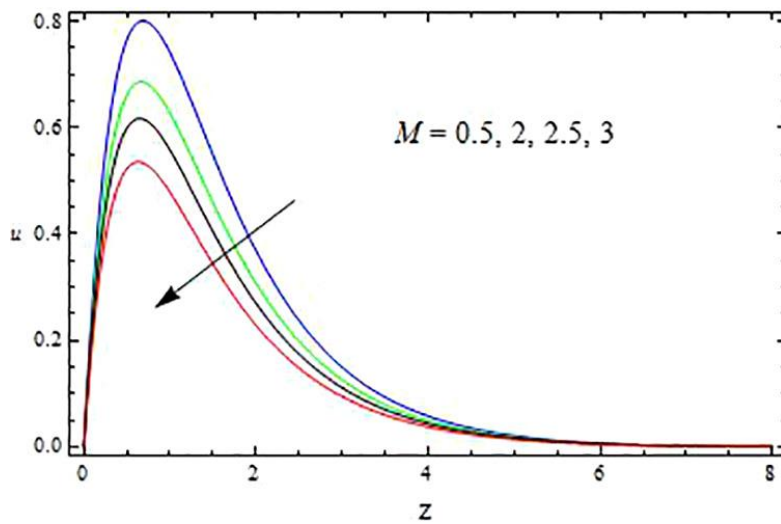


Fig. .4: The velocity profile for u against M

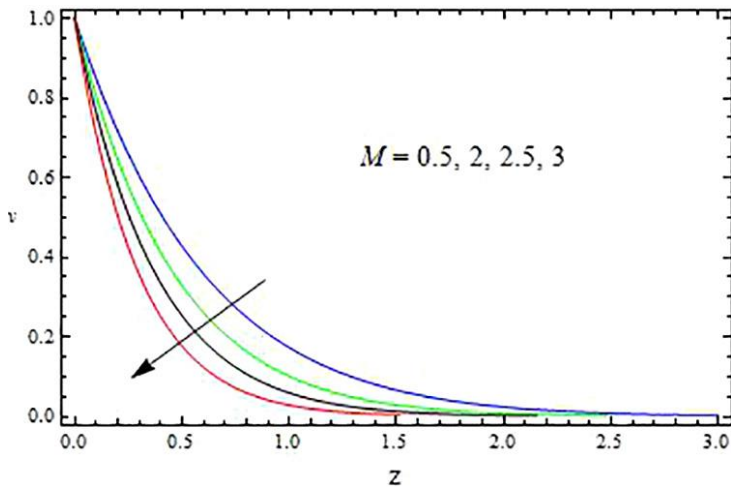


Fig.5 : The velocity profile for v against M

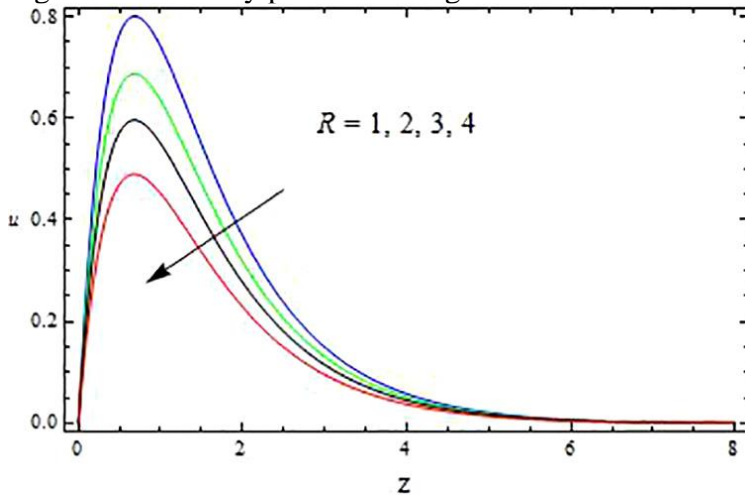


Fig.6: The velocity profile for u against R

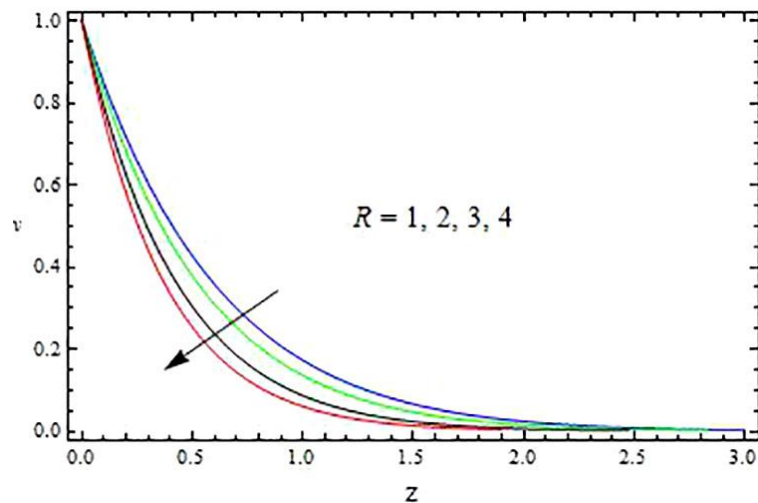


Fig.7. : The velocity profile for v against R

Table.1 Shear Stress (τ) at $\eta=1$ $P=0.71$, $\alpha=2$, $\beta=0.5$, $x=\pi/4$, $t=\pi/4$, $N_1=4$

G/ τ	I	II	III	IV	V
5×10^2	-0.04916	1.082563	1.331555	3.701947	7.284086
10^3	-1.37451	0.416935	0.998004	3.336792	7.188192
3×10^3	-1.82769	0.175573	0.87363	2.649002	6.998722
-5×10^2	4.788339	3.501522	2.541088	4.445451	7.478382
-10^3	8.295419	5.253588	3.416752	4.883779	7.576783
-3×10^3	17.48143	9.84365	5.711047	5.744379	7.776292

Table.2 Shear Stress (τ) at $\eta=-1$ $P=0.71$, $\alpha=2$, $\beta=0.5$, $x=\pi/4$, $t=\pi/4$, $N_1=4$

G/ τ	I	II	III	IV	V
5×10^2	0.074145	-0.84007	-1.61531	-3.2391	-6.81185
10^3	1.384482	-0.18195	-1.28551	-2.88109	-6.71972
3×10^3	1.807631	0.0444	-1.16864	-2.2076	-6.53778
-5×10^2	-4.73333	-3.24402	-2.81734	-3.9983	-6.99862
-10^3	-8.2254	-4.98858	-3.68925	-4.39948	-7.09325
-3×10^3	-17.3814	-9.56363	-5.97604	-5.24579	-7.28523

R	35	70	140	35	35
M	2	2	2	5	10

Table.3 Shear Stress (τ) at $\eta=1$ $P=0.71$, $R=35$, $M=2$, $\alpha=2$, $\beta=0.5$, $x=\pi/4$, $t=\pi/4$

G/ τ	I	II	III	IV	V	VI
5×10^2	0.00361	0.108604	-0.20916	0.161831	0.155393	-0.08122
10^3	-1.26833	-1.20378	-1.53451	-1.16758	-1.18358	-1.43094
3×10^3	-1.61456	-1.59075	-1.98769	-1.6289	-1.66402	-1.93291
-5×10^2	4.734257	4.859859	4.628339	5.00745	5.020125	4.805008
-10^3	8.187914	8.333868	8.135419	8.518593	8.540822	8.336455
-3×10^3	17.26697	17.45367	17.32143	17.71273	17.7541	17.57126

Table.4. Shear Stress (τ) at $\eta=-1$ $P=0.71$, $R=35$, $M=2$, $\alpha=2$, $\beta=0.5$, $x=\pi/4$, $t=\pi/4$

G/ τ	I	II	III	IV	V	VI
5×10^2	0.021384	0.126386	-0.08586	0.293156	0.305594	0.090212
10^3	1.278299	1.423749	1.224482	1.607555	1.629549	1.424917
3×10^3	1.594496	1.78069	1.647631	2.038835	2.079959	1.896851
-5×10^2	-4.67925	-4.59485	-4.89333	-4.52244	-4.52912	-4.76599
-10^3	-8.1179	-8.05385	-8.3854	-8.01857	-8.0348	-8.28244
-3×10^3	-17.167	-17.1437	-17.5414	-17.1827	-17.2181	-17.4872

N_1	0.4	1.0	4.0	5.0	10.0	100.0
-------	-----	-----	-----	-----	------	-------

Table.5. Nusselt number (Nu) at $\eta=1$ $P=0.71$, $\alpha=2$, $\beta=0.5$, $x=\pi/4$, $t=\pi/4$, $N_1=4$

G/Nu	I	II	III	IV	V
5×10^2	0.1415	0.2442	-0.0219	0.3534	0.3558
10^3	0.1461	0.2465	-0.0208	0.3543	0.356
3×10^3	0.1554	0.2511	-0.0185	0.3562	0.3564
-5×10^2	0.1323	0.2396	-0.0242	0.3516	0.3554
-10^3	0.1276	0.2373	-0.0254	0.3507	0.3551
-3×10^3	0.1178	0.2326	-0.0277	0.349	0.3547

Table.6 Nusselt number (Nu) at $\eta=-1, P=0.71, \alpha=2, \beta=0.5, x=\pi/4, t=\pi/4, N_1=4$

G/Nu	I	II	III	IV	V
5×10^2	-1.61056	-1.49938	-1.76177	-1.3847	-1.38107
10^3	-1.62678	-1.50554	-1.76437	-1.38531	-1.38103
3×10^3	-1.67603	-1.5217	-1.7705	-1.38675	-1.38095
-5×10^2	-1.59328	-1.49077	-1.75746	-1.38368	-1.38115
-10^3	-1.59184	-1.48826	-1.75576	-1.38328	-1.3812
-3×10^3	-1.60304	-1.50677	-1.77322	-1.39269	-1.3913
R	35	70	140	35	35
M	2	2	2	5	10

Table.7 Nusselt number (Nu) at $\eta=1, P=0.71, R=35, M=2, \alpha=2, \beta=0.5, x=\pi/4, t=\pi/4$

G/Nu	I	II	III	IV	V	VI
5×10^2	-0.9702	-0.8656	-0.0185	0.4082	0.5224	-1.6191
10^3	-0.9957	-0.3236	-0.0139	0.4137	0.5297	-1.619
3×10^3	-1.0719	-0.3494	-0.0046	0.4254	0.5462	-1.619
-5×10^2	-0.9396	-0.3077	-0.0277	0.3978	0.5095	-1.6192
-10^3	-0.9335	-0.3076	-0.0324	0.3927	0.5037	-1.6192
-3×10^3	-0.9381	-0.3148	-0.0422	0.3826	0.493	-1.6293

Table.8. Nusselt number (Nu) at $\eta=-1, P=0.71, R=35, M=2, \alpha=2, \beta=0.5, x=\pi/4, t=\pi/4$

G/Nu	I	II	III	IV	V	VI
5×10^2	-0.9702	-0.8656	-0.0185	0.4082	0.5224	0.4064
10^3	-0.9957	-0.3236	-0.0139	0.4137	0.5297	0.4152
3×10^3	-1.0719	-0.3494	-0.0046	0.4254	0.5462	0.436
-5×10^2	-0.9396	-0.3077	-0.0277	0.3978	0.5095	0.3913
-10^3	-0.9335	-0.3076	-0.0324	0.3927	0.5037	0.3848
-3×10^3	-0.9381	-0.3148	-0.0422	0.3826	0.493	0.3736

N_1	0.4	1.0	4.0	5.0	10.0	100.0
-------	-----	-----	-----	-----	------	-------

The Shear stress at the boundaries $\eta=\pm 1$ are evaluated for different variations of G, R, M, and N_1 are presented in Tables. 1 – 4. It is found that the stress at $\eta=1$ is negative in the heating case and positive in the cooling case for $R=35$. For higher $R \geq 70$ the stress is positive for all G, while at $\eta=-1$ the stress is positive for $G > 0$ and negative for $G < 0$. The magnitude of stress at $\eta=\pm 1$ increases with increase in $|G|$, R and M (Tables. 1 & 2).

The effect of the radiation parameter N_1 on τ is to enhance its magnitude for all G fixing the other parameters (Tables 3 & 4).

The Nusselt number (Nu) which measures the rate of heat transfer at the boundaries has been numerically evaluated for different values of the governing parameters. It is found that the Nusselt number is positive at both the walls for all variations. $|Nu|$ at $\eta=\pm 1$ enhances with $G > 0$ and depreciates with $G < 0$. An increase in M or R reduces ‘Nu’ at both the walls in the heating case and enhance in the cooling case (Tables. 5 & 6). From Tables. 7 & 8. we find that at $\eta=1$ the rate of heat transfer reduces with $N_1 \leq 5$ and for higher $N_1 > 5$ we find an enhancement in ‘Nu’, while at $\eta=-1$, $|Nu|$ experiences an enhancement with N_1 for all G .

6. References:

[1] J. Hartmann, Hg-dynamics I theory of the laminar flow of an electrically conductive liquid in a homogenous magnetic field, Det Kongelige Danske Videnskabernes Selskab Mathematisk-fysiske Meddelelser 15 (1937) 1–27.



- [2] V.V.S. Murty, A. Gupta, N. Mandloi, A. Shukla, Evaluation of thermal performance of heat exchanger unit for parabolic solar cooker for off-place cooking, *Indian J.Pure Appl. Phys.* 45 (2007) 745–748.
- [3] N.K. Raja, M.S. Khalil, S.A. Masood, M. Shaheen, Design and manufacturing of parabolic trough solar collector system for a developing country Pakistan, *J. Am.Sci.* 7 (2011) 365–372.
- [4] R. Muthucumaraswamy, E. Geetha, Effects of parabolic motion on an isothermal vertical plate with constant mass flux, *Ain Shams Eng. J.* 5 (2014) 1317–1323.
- [5] N.S. Akbar, S. Nadeem, R.U. Haq, S. Ye, MHD stagnation point flow of Carreau fluid toward a permeable shrinking sheet: dual solutions, *Ain Shams Eng. J.* 5 (2014) 1233–1239.
- [6] M. Sheikholeslami, D.D. Ganji, M. Gorji-Bandpy, Soheil Soleimani, Magnetic field effect on nanofluid flow and heat transfer using KKL model, *J. Taiwan Inst. Chem.Eng.* 45 (2014) 795–807.
- [7] M. Sheikholeslami, D.D. Ganji, M.M. Rashidi, Magnetic field effect on unsteady nanofluid flow and heat transfer using Buongiorno model, *J. Magn. Magn. Mater.* 416 (2016) 164–173.
- [8] M. Sheikholeslami, M. Gorji-Bandpy, D.D. Ganji, MHD free convection in an eccentric semi-annulus filled with nanofluid, *J. Taiwan Inst. Chem. Eng.* 45 (2014) 1204–1216.
- [9] M. Sheikholeslami, R. Ellahi, Three dimensional mesoscopic simulation of magnetic field effect on natural convection of nanofluid, *Int. J. Heat Mass Transf.* 89 (2015) 799–808.
- [10] M. Sheikholeslami, K. Vajravelu, M.M. Rashidi, Forced convection heat transfer in a semi annulus under the influence of a variable magnetic field, *Int. J. Heat Mass Transf.* 92 (2016) 339–348.
- [11] M. Sheikholeslami, A.J. Chamkha, Electrohydrodynamic free convection heat transfer of a nanofluid in a semi-annulus enclosure with a sinusoidal wall, *Numer.Heat Transfer, Part A* 69 (2016) 781–793.
- [12] M. Veera Krishna, Radiation-absorption, chemical reaction, Hall and ion slip impacts on magnetohydrodynamic free convective flow over semi-infinite moving absorbent surface *Chinese Journal of Chemical Engineering* 34 (2021) 40–52.
- [13] M.R.S.N. Syed, T. Muhammad, S. Saleem, H.M. Kim, Significance of non-uniform heat generation/absorption in hydromagnetic flow of nanofluid due to stretching/shrinking disk, *Physica A: Stat. Mech. Applicat.* 553 (2020),
- [14] S. Saleem, B. Heidarshenas, An investigation on exergy in a wavy wall microchannel heat sink by using various nanoparticles in fluid flow: two-phase numerical study, *J. Therm. Anal. Calorim.* 145 (2021) 1599–1610
- [15] M. Nazeer, S. Saleem, F. Hussain, S. Iftikhar, A. Al-Qahtani, Mathematical modeling of bio-magnetic fluid bounded by ciliated walls of wavy channel incorporated with viscous dissipation: discarding mucus from lungs and blood streams, *Int. Communicat. Heat Mass Transfer* 124 (2021),
- [16] A. Al-Zubaidi, M. Nazeer, K. Khalid, S. Yaseen, S. Saleem, F. Hussain, Thermal analysis of blood flow of Newtonian, pseudo-plastic and dilatant fluids through an inclined wavy channel due to metachronal wave of cilia, *Adv. Mech. Eng.* 13 (9)(2021) 1–12,.
- [17] M. Nazeer, S. Saleem, F. Hussain, M.U. Rafiq, Numerical solution of gyrotactic microorganism flow of nanofluid over a Riga plate with the characteristic of chemical reaction and convective condition, *Waves Random Complex Media* (2022),
- [18] H.V. Kiranakumar, R. Thejas, C.S. Naveen, M.I. Khan, G.D. Prasanna, S. Reddy, M. Oreijah, K. Guedri, O.T. Bafakeeh, M. Jameel, A review on electrical and gassensing properties of reduced graphene oxide-metal oxide, nanocomposites, *Biomass Convers. Bioref.* (2022),
- [19] M.I. Khan, T. Hayat, M. Waqas, M.I. Khan, A. Alsaedi, Entropy generation minimization (EGM) in nonlinear mixed convective flow of nanomaterial with joule heating and slip condition, *J. Mol. Liq.* 256 (2018) 108–120,
- [20] M.I. Khan, M.I. Khan, M. Waqas, T. Hayat, A. Alsaedi, Chemically reactive flow of Maxwell liquid due to variable thicked surface, *Int. Communicat. Heat Mass Transfer* 86 (2017) 231–238.



- [21] T. Hayat, M.I. Khan, M. Waqas, A. Alsaedi, Mathematical modeling of non-Newtonian fluid with chemical aspects: a new formulation and results by numerical technique, *Colloids Surf. A Physicochem. Eng. Asp.* 518 (2017)263–272,
- [22] T. Hayat, M.I. Khan, M. Waqas, A. Alsaedi, Effectiveness of magnetic nanoparticles in radiative flow of Eyring-Powell fluid, *J. Mol. Liq.* 231 (2017) 126–133,
- [23] A. Abbasi, W. Farooq, E.S.M. Tag-ElDin, S.U. Khan, M.I. Khan, K. Guedri, S. Elattar, M. Waqas, A.M. Galal, Heat transport exploration for hybrid nanoparticle (Cu,Fe₃O₄)—based blood flow via tapered complex wavy curved channel with slip features, *Micromachines* 13 (2022) 1415
- [24] K. Vajravelu, K.V. Prasad, *Keller Box Method and its Application 2*, De Gruyter Higher Education Press, 2014, pp. 1–412.